Clin Oral Invest (2013) 17:441–448
DOI 10.1007/s00784-012-0718-0

ORIGINAL ARTICLE

An optimized video system for augmented reality in endodontics: a feasibility study

D. D. Bruellmann · H. Tjaden · U. Schwanecke · P. Barth

Received: 12 December 2011 / Accepted: 6 March 2012 / Published online: 31 March 2012

Abstract
Objectives We propose an augmented reality system for the reliable detection of root canals in video sequences based on a *k*-nearest neighbor color classification and introduce a simple geometric criterion for teeth.
Material and methods The new software was implemented using C++, Qt, and the image processing library OpenCV. Teeth are detected in video images to restrict the segmentation of the root canal orifices by using a *k*-nearest neighbor algorithm. The location of the root canal orifices were determined using Euclidean distance-based image segmentation. A set of 126 human teeth with known and verified locations of the root canal orifices was used for evaluation.
Results The software detects root canals orifices for automatic classification of the teeth in video images and stores location and size of the found structures. Overall 287 of 305 root canals were correctly detected. The overall sensitivity was about 94 %. Classification accuracy for molars ranged from 65.0 to 81.2 % and from 85.7 to 96.7 % for premolars.
Conclusion The realized software shows that observations made in anatomical studies can be exploited to automate real-time detection of root canal orifices and tooth classification with a software system.
Clinical relevance Automatic storage of location, size, and orientation of the found structures with this software can be used for future anatomical studies. Thus, statistical tables with canal locations will be derived, which can improve anatomical knowledge of the teeth to alleviate root canal detection in the future. For this purpose the software is freely available at: http://www.dental-imaging.zahnmedizin.uni-mainz.de/.

Keywords Augmented reality · Automatic feature detection · Root canal orifices

Electronic supplementary material The online version of this article (doi:10.1007/s00784-012-0718-0) contains supplementary material, which is available to authorized users.

D. D. Bruellmann (✉)
Department of Oral Surgery, University Medical Center,
Johannes Gutenberg-University,
Mainz, Germany
e-mail: bruellmd@uni-mainz.de

H. Tjaden · U. Schwanecke · P. Barth
Department of Design, Computer Science and Media,
RheinMain University of Applied Sciences,
Wiesbaden, Germany

U. Schwanecke
e-mail: ulrich.schwanecke@hs-rm.de

P. Barth
e-mail: peter.barth@hs-rm.de

Introduction

Augmented reality (AR) technology combines intra-oral cameras with dedicated image processing software. It has been shown to be useful in video-assisted e-Learning applications in medical and dental education and has been reported as a successful method of teaching anatomy to students while providing them with additional visual information [1–4]. The intraoperative visualization of information appears to be one of the most promising fields of application for augmented reality in medicine [5]. The acceptance of augmented reality technology in dental diagnosis and dental education can be greatly increased by employing a solution using standard intra-oral or microscope cameras connected to a standard computer. Dentists generally use loupes or microscopes in order to detect all root canal orifices. The use of well-focused illumination and

magnification devices has improved the dentist's ability to increase the effectiveness and quality of endodontic therapy [6]. Diagnosis based on image analysis with digital intra-oral cameras is usually aimed at plaque and caries detection, but only a few studies have been conducted to assess their use for endodontic diagnosis [7–9].

In this paper, we focus on supporting diagnosis, in particular the automatic detection of root canal orifices. First, we present an efficient, highly optimized *k*-nearest neighbor color classification approach for real-time detection of root canals in video sequences obtained by intra-oral video cameras. Second, we present a simple geometric criterion for tooth classification based on the mutual positions of the detected roots. Finally, we describe an integrated AR system based on the presented methods that augments video images with the extracted information in real-time, demonstrating the efficiency of our detection and classification algorithm. An anatomical study revealed that the color distribution and the geometry of the pulp chamber floor follow certain laws [10]. The floor of the pulp chamber mostly appears as a darker color than the surrounding dentinal walls. This color difference creates a distinct junction where the walls and the floor of the pulp chamber meet. Root canals are always located at the junction of the walls and floor. Further, the root canal orifices are generally equidistant from the circumference of the tooth at the level of cemento-enamel junction. With a derivative of these observations of color distribution in the pulp chamber floor the detection of root canal orifices has already been realized with standard C-Mount CCD cameras mountable on different microscopes [11]. To this end, a simplified minimum distance classification using Euclidean distance-based image segmentation for fast detection of these anatomical structures has been used, but no classification of the tooth type, nor adaptable color classification or storage of anatomical landmark location for statistical use has been implemented so far [12].

The aim of this study was to develop and to test a new software system for the location of the root canal orifices and classification of the teeth.

Methodology

The new software was implemented using C++, Qt, and the image processing library OpenCV. Teeth are detected in video images to restrict the segmentation of the root canal orifices by using a *k*-nearest neighbor algorithm. The location of the root canal orifices were determined using Euclidean distance-based image segmentation. A set of 126 human teeth with known and verified locations of the root canal orifices was used for evaluation.

Detection of tooth and root canal orifices

The segmentation of a certain pixel P with RGB-color-vector (P_R, P_G, P_B) depends on the Euclidean distance of its intensity to the intensity of the darkest pixel with color-vector (X_R, X_G, X_B). A pixel is labeled as root canal, if the Euclidean distance to (X_R, X_G, X_B) is smaller than a predefined threshold s:

$$(X_R - P_R)^2 + (X_G - P_G)^2 + (X_B - P_B) < s^2$$

This segmentation assay exploits the visual properties of the root canal orifices, being the deepest regions in the pulp chamber floor; the canal orifices are always the darkest regions of the image within the cavity boundary [11]. The contours of root canal orifices always appear solid as well as round, elliptical, or oval.

The definition of color classes is interactively provided by identifying relevant regions on an image by the user. Based on the results of the root canal detection, we classify teeth with the help of geometric criteria. First, the teeth have to be detected in the images in order to restrict the segmentation of the root canal orifices to their typical anatomical region. A color classification *k*-nearest neighbor algorithm is used for the segmentation of the teeth [13]. This algorithm determines the color class for each pixel in an image. The idea is to find the *k*-nearest neighbors of the pixel's color in the present color classes within a maximal radius. Here, proximity is measured using the Euclidean metric in color-space. A color class is a set of color values with a corresponding index that describes an image region. For tooth detection, a color class is a collection of color values that most likely belong to a tooth region. If the absolute majority of a pixel's neighbors in the colors of the classes belongs to the same class, the pixel itself gets assigned to that class. We let the user interactively define the color classes by marking samples of the regions to detect. The user picks rectangular regions containing colors of a desired class in a sample video image (see Fig. 1, left). Based on the samples, a kd-tree is generated that encodes the spatial structure of the color class and allows for fast retrieval. We use an optimized kd-tree implementation [14].

With the resulting kd-tree, the *k*-nearest neighbors within the color classes of any color value can be found efficiently. Because the tree sorts the color values according to their location in the color-space, many nodes can be ignored during the recursive tree search [15]. Although this method is very fast, it does not suffice for real-time analysis of an entire image. Note that the color classes are not widely changing during the tooth detection, which we use to speed up the color classification process. We define color classes in advance and do not change them while the detection proceeds. Thus, a look-up table of the *k*-nearest neighbors (i.e., the resulting color class) of all 16 million possible

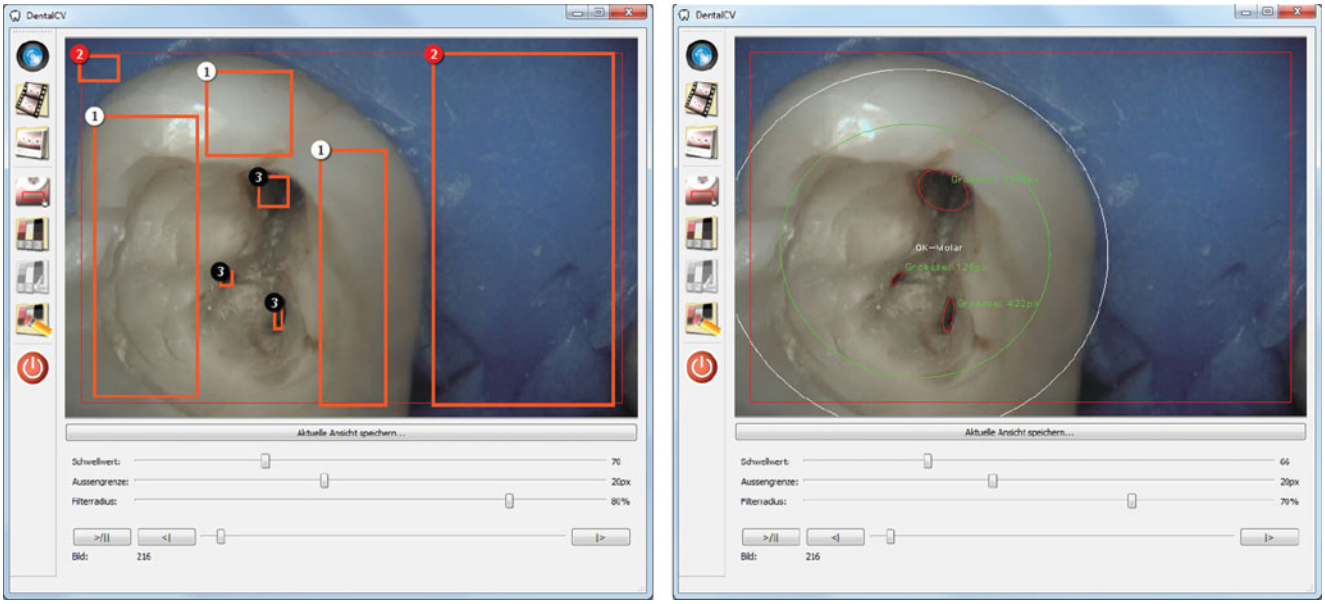

Fig. 1 Graphical user interface of the developed software. *Left* Creation of color classes with rectangular user selections in a sample image. The corresponding class index is displayed in the upper-left corner of the selection rectangle. *Right* Video image of a tooth and augmented information

colors with the respective color classes could be created. A look-up table reduces the search for the neighbors of any pixel in an image to a single array access. Such a look-up table could have been created in an initial step. Unfortunately, it takes a long time to create the table. Tests with a 2.66 GHz Intel CPU show that approximately 30 min are needed to construct the complete look-up table. But since most of the colors will not be needed, the table is only sparsely populated. Therefore, it makes sense to fill the look-up table gradually by memorizing each new color value and its corresponding class whenever it first appears. With this method, the first few images will be processed rather slowly, because most color values are not yet in the look-up table. Tests showed that after 20–30 images almost no new color values occur and therefore most color classes can be determined with a single access into the look-up table. After the color class for every pixel in an image is determined, connected regions containing pixels attributed to the color class for teeth are labeled using line-wise run-length encoding and an efficient union-find algorithm [16]. Characteristic quantities such as surface area, coordinates of the center of mass, orientation, and expansion can be calculated for each connected region with help of statistical moments [17]. Thereby, the surface area is used to determine the largest tooth region because it is assumed that this region is most likely the actual tooth of interest and not a neighboring tooth or a falsely segmented region. The center of mass is used to describe the position of a region. Knowing the orientation and the expansion of a tooth, an ellipse approximating the shape of the tooth can be calculated (see Fig. 2). We use this ellipse as a very efficient filter for the segmented root canal regions because it mimics the general shape of a tooth quite accurately. Then the location of the root canal orifices can be determined with help of a simplified minimum distance classification by means of Euclidean distance-based image segmentation.

An additional anatomical constraint helps to further restrict the segmentation of the canal orifices into the center of the tooth: root canals are generally equidistant located to the circumference of the tooth at the level of cemento-enamel junction [10]. That fact can be approximated by using a second smaller ellipse positioned inside the segmented tooth.

Classification of tooth types

Based on the calculated parameters and the number of root canal orifices, we can distinguish between the following six tooth types as depicted in Fig. 3. The first criterion used to distinguish between the types of teeth is the number of the canal orifices. There are two clear cases. When two orifices are found, we always determine the tooth type as first upper premolar and, in the case of four found orifices, as upper molar. In the case of only one canal orifice, the aspect ratio of the main axes is used as the significant criterion. If the main axes are approximately equal in length, it is most probably a premolar. Otherwise, if the axes lengths are rather unequal, the proposed tooth type is incisor. If there are three root canals, it needs to be decided whether it is an upper or a lower molar. This choice is made according to the properties of the triangle given by the centers of the orifice regions. The observation leading to this approach is that there is always one canal orifice that is noticeably larger than the other two. The distance of this largest canal orifice to the perpendicular bisector of the side between the two smaller ones varies consistently between the two possible tooth types. When looking at an upper molar the distance is

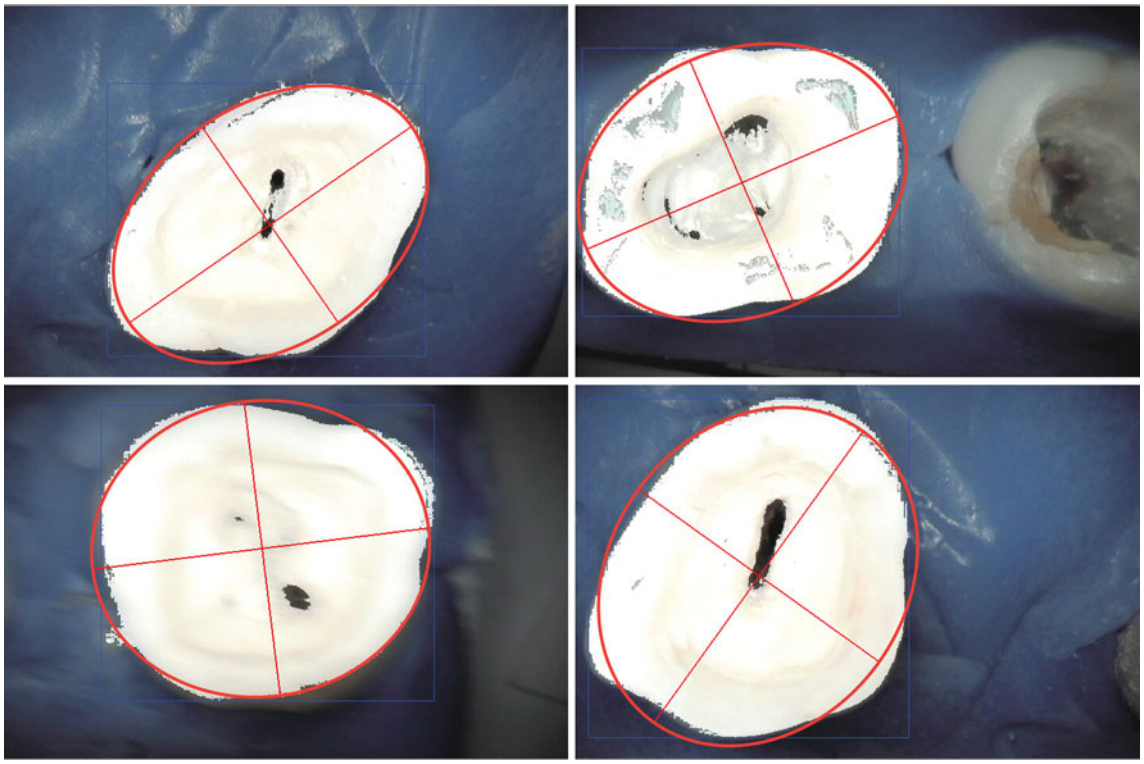

Fig. 2 Visualization of the orientation and extension of a region. The main axes and the bounding ellipse are displayed in *red*

rather large whereas it is rather small in the case of a lower molar. To obtain a geometric criterion that is more robust against the measured size of the orifices, we used the relationship between the barycenter of the triangle and the center of its circumscribed circle as a criterion to differentiate between these two cases. The closer these two points are together, the more likely it is that the observed tooth is a lower molar and, vice versa, an upper molar.

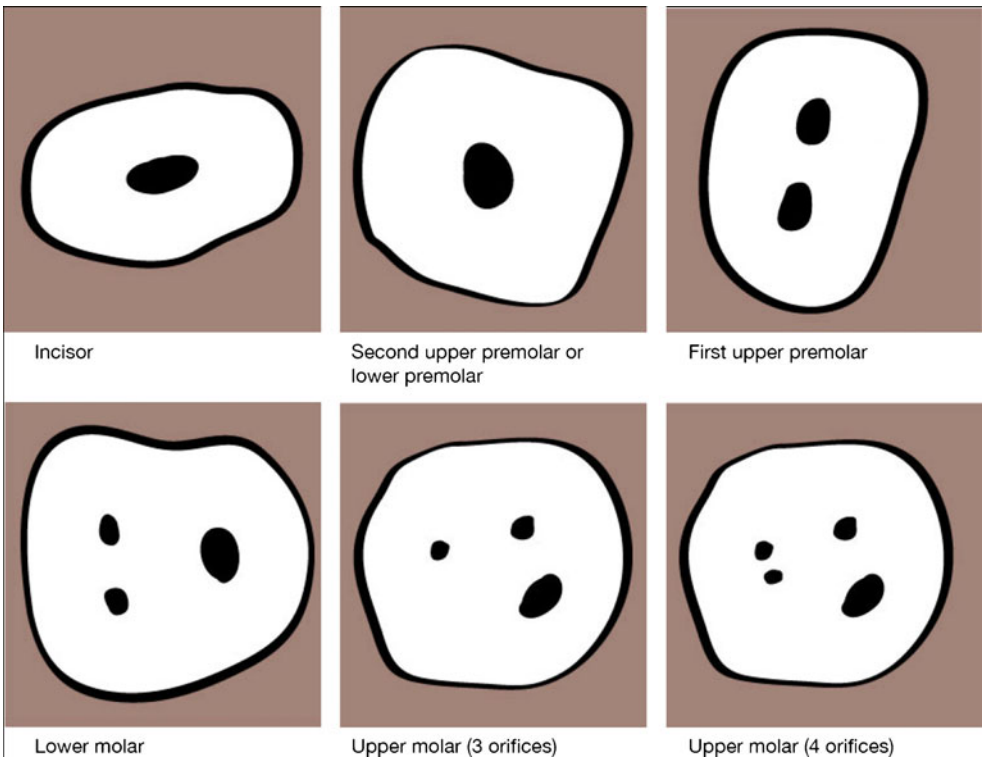

Fig. 3 Schematic top views of the human tooth types that can be distinguished by our system. *Incisors* with one canal orifice and a longish shape, *premolars* with one root canal and a roundish shape, *first upper premolars* with two canal orifices, *upper molars* with three or four canal orifices and *lower molars* with three canal orifices. Natural exceptions such as molars with five root canals are being ignored

Table 1 Characteristics used to distinguish the different tooth types

Tooth type	Incisor	Upper first premolar	Other premolars	Lower molar	Upper molar
Nr. of orifices	1	2	1	3	3–4
Aspect ratio main axis	>1.5		≤1.5		
Triangle criterion				$R_{(DES)}\leq 2$	$R_{(DES)}>2$

The barycenter of a triangle with vertices $A = (x_1, y_1)^T$, $B = (x_2, y_2)^T$ and $C = (x_3, y_3)^T$ is given by:

$$S = \frac{1}{3}(A + B + C)$$

Using the fact that the equation of the circumscribed circle containing the three vertices A, B, C can be found by solving:

$$|M| = 0 \quad with\ M = \begin{pmatrix} x^2 + y^2 & x & y & 1 \\ x_1^2 + y_1^2 & x_1 & y_1 & 1 \\ x_2^2 + y_2^2 & x_2 & y_2 & 1 \\ x_3^2 + y_3^2 & x_3 & y_3 & 1 \end{pmatrix}$$

The center U as well as the radius r_u of this circle are given by:

$$U = (x_u, y_u)^T = \left(\frac{M_{12}}{2M_{11}}, \frac{M_{12}}{2M_{11}}\right)^T$$

and

$$r_u = \sqrt{x_u^2 + y_u^2 - \frac{M_{14}}{M_{11}}}$$

with M_{1j} being the minors of M. Because the distance between the camera and the teeth being filmed can vary, the relation between the centers must be measured scale-invariant. By defining a ratio based on the barycenter of the triangle and its circumscribed circle, we obtain an affine invariant characteristic for each tooth class. Therefore, we consider the two intersections D and E of the Euler line containing S and U with the circumscribed circle of the triangle. These intersections are given by

$$D = U - r_u \frac{U - S}{\|U - S\|}$$

and

$$E = U - r_u \frac{U - S}{\|U - S\|}$$

U is always the midpoint between D and E, but S varies depending on the shape of our triangle defined by the position of the root canals. Thus, we can calculate the affine invariant cross ratio

$$R_{(DES)} = \frac{\|D - S\|}{\|S - E\|}$$

of the collinear points D, S and E as a characteristic of a tooth. If $R_{(DES)}=1$ we know that S is equidistant to D and E, and the triangle is equilateral. Increasing asymmetric triangles lead to larger results of the division ratio. A result of the cross ratio $R_{(DES)}<2$ indicates correctly that the tooth in question is a lower molar. Otherwise, if $R_{(DES)}\geq 2$ it is an upper molar. Table 1 provides an overview of the characteristics used to distinguish the different tooth types, while Fig. 4 depicts video images augmented with the information determined by our algorithm. Classification results were tested in real-time with a Duerr VistaCam Digital on 126 extracted human molars, prepared as described in a previous study [11].

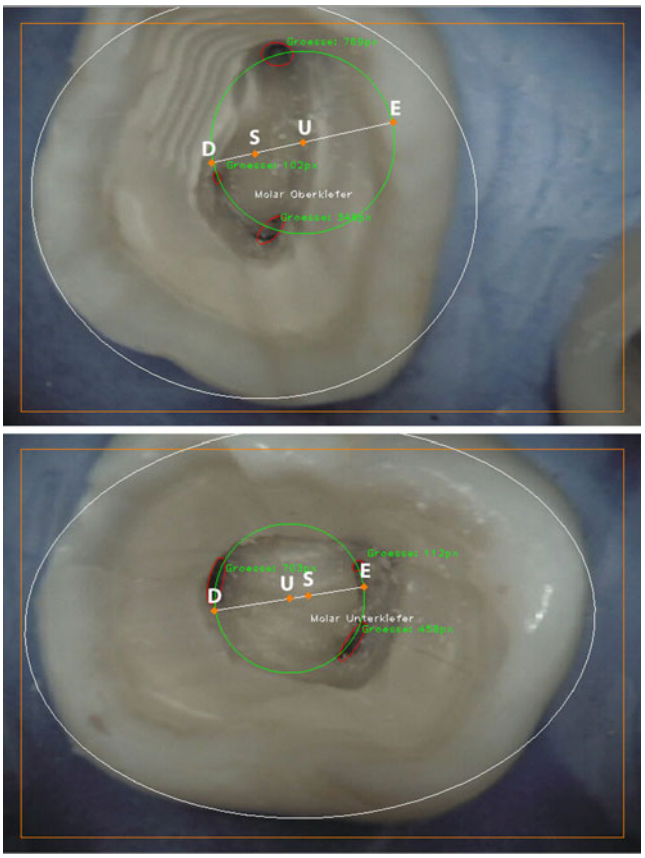

Fig. 4 Two images augmented with different determined characteristics. *Right* An upper molar. *Left* A lower molar. We consider the two intersections D and E of the Euler line containing S and U with the circumscribed circle of the triangle formed by the centers of the orifice regions

Table 2 Different types of tooth and corresponding performance for orifice detection

	Quantity	Orifices indicated	Orifices verified	False negative	False positive	Right positive	Sensitivity (%)
Total	126	296	305	18	9	287	94
Upper molar with 4 orifices	7	27	28	2	1	26	93
Upper molar with 3 orifices	32	90	96	7	1	89	95
Lower molar	40	115	120	9	4	111	93
First upper premolar	14	31	28	0	3	28	100
Other premolars	28	28	28	0	0	28	100
Incisor	5	5	5	0	0	5	100

Implementation

Our system is implemented in Microsoft Visual C++ 8.0, Microsoft Corp., Redmond, USA with additional libraries for image processing and an UI-Toolkit. We used the GUI framework Qt (http://qt.nokia.com/) and the open source image processing library OpenCV 2.1(http://sourceforge.net/projects/opencvlibrary/).

Users can load images as well as videos or start a video stream from a camera. The system processes each single image by performing the described algorithm. Because part of this process is based on the *k*-nearest neighbor algorithm, a configuration file containing the color classes is needed. These files can be created, saved, and loaded with the software. The software also offers functions such as video controls and the possibility of saving current calculations. Not only can the augmented image be saved, but also a text file containing the measured values (positions and orientations of the orifices and the tooth as well as its type).

Results

The software detects root canals orifices for automatic classification of the teeth in video images and stores location, size, and orientation of the found structures. The system was tested towards detection accuracy on a simulated in vitro model. For the simulated data set, color classes for soft tissue (simulated rubber dam) as well as teeth (dentin and enamel of extracted human molars) were defined in two images for four corresponding areas. The detection accuracy was evaluated against a set of 126 human teeth with known and histologically verified locations of the root canal orifices. Overall 287 of 305 root canals were correctly detected as positive, and the overall sensitivity was about 94.0 %. The detailed result for the different tooth types is listed in Table 2.

Color classes for the in vitro data were defined in two images not contained in the dataset used for testing on four locations for the surrounding and four locations for the teeth, respectively. Detection is very fast and allows real-time usage. Each step of the calculation process only takes a few milliseconds. When processing an image sequence from a camera or a video file, the performance of the system improves quickly for each new observation. After about 25 images have been processed, enough color classes have been found in order to process the images in almost real-time (<40 ms). The classification of the tooth type takes less than 1 ms for each image. The times have been measured on a desktop computer with an Intel Core i7-920 Processor (2.66 GHz) and 4 GB DDR3-1066 RAM. The software shows different classification performance for the different classes of teeth and is able to distinguish with 90 % accuracy between upper and lower molars (see Table 3).

Discussion

The software system presented here uses algorithms to segment the visually darker regions in which the root canal

Table 3 Different tooth populations and related classification results

	Upper molar (4 orifices)	Upper molar (3 orifices)	Lower molar	First upper premolar	Other premolar	Incisor
Total number	7	32	40	14	28	5
Correct classified	5	26	26	12	27	2
Incorrect classified	2	6	14	2	1	3
Correct (%)	71.4	81.2	65.0	85.7	96.4	40.0

orifices are to be expected. The software approximates the rule that root canals are generally equidistant from the circumference of the tooth at the level of the cemento-enamel junction. This is the basic principle for a system using more of the anatomical observations made in recent literature to improve the automatic detection of root canal orifices [10, 18]. This method for identifying root canals in endodontically accessed teeth provides a stable detection of the sought after anatomical landmarks and is sufficiently robust against misdetections of cast shadows in the neighborhood. Stable and accurate identification of the color classes for the detection of the teeth in the images via the *k*-nearest neighbor algorithm requires picking of the color classes for gum and teeth by the user. This means, that observations of pulp stones, calcifications and other common obliterations could be implemented in that software. Generally, carious lesions and fillings should be removed completely prior to endodontic treatment in order to avoid the missing of anatomical structures and to prevent re-infection by tissue remnants or coronal leakage of probably insufficient fillings. However, *k*-nearest neighbor classification is very stable and able to be trained on a high number of color classes. So we think unusual colors can be included into the classification dataset by the user.

As most endodontic treatment has to be conducted under completely sealed conditions, which can be only provided by the use of rubber dams, we assume that it suffices that the colors of the dam and its clamp has to be defined once for each rubber dam brand. Because the color of teeth do not vary much on the camera images, we hope to show in the future that training of tooth colors performed on a tooth color chart or a few videos initially taken during the setup of the software and the camera system can be sufficient. The classification of tooth types requires a correct detection of all of the root canal orifices.

A missed root canal or an additional falsely detected root canal will result in a misclassification of the tooth type. This was especially true for lower molars because, in this case, the mesiobuccal canal and its lingually located neighbor originated in a deep isthmus which was segmented as one canal orifice by the software. Thus, a low correct classification of 65 % was achieved for this type of tooth. Further, a more stable classification rule has to be evolved in order to classify anterior teeth more accurately because this type of tooth was only correctly classified in 40 % of the cases. However, only a small number of five anterior teeth were available for evaluation in this study. Another problem for the correct classification of the tooth type is that the angulation between the detected structures can change with the angulation of the camera. Therefore, the correct angulation between root canal orifices can only be obtained if 3D images are used. If the root canal orifices can be detected as stable landmarks in video images, three-dimensional reconstructions of the operation site via intra-oral cameras might be possible in the near future [19–21]. Because our proposed system automatically detects reproducible landmarks, three-dimensional reconstruction may be possible on site in real-time. This additional three-dimensional information can then be used for the detection of isthmi between the root canal orifices or the computer aided design of restoration posts prior to the prosthodontic care of the tooth after root canal treatment.

Conclusion

This paper shows that observations made in anatomical studies can be exploited to automate real-time detection of root canal orifices and tooth classification with a software system. The implementation of defined color classes is feasible and functional for the implementation of further color phenomena detectable in the pulp chamber floor. Automatic storage of location, size, and orientation of the found structures with this software can be used for future anatomical studies.

Acknowledgments This article contains parts of the bachelor thesis of Henning Tjaden. Further, the authors declare that there are no conflicts of interest, nor financial relations to any commercial corporation or products.

References

1. Edwards P, King A, Hawkes D et al (1999) Stereo augmented reality in the surgical microscope. Stud Health Technol Inform 62:102–108
2. Tse B, Harwin W, Barrow A, Quinn B, San Diego J, Cox M (2010) Design and development of a haptic dental training system – Haptel. In: Kappers A, van Erp J, Bergmann-Tiest W, van der Helm F (eds) Haptics: generating and perceiving tangible sensations, 1st edn. Springer, Heidelberg, pp 101–108
3. Sutherland L, Middleton P, Anthony A et al (2006) Surgical simulation: a systematic review. Ann Surg 243:291–300
4. Thomas R, John N, Delieu J (2010) Augmented reality for anatomical education. J Vis Commun Med 33:6–15
5. Birkfellner W, Figl M, Huber K et al (2002) A head-mounted operating binocular for augmented reality visualization in medicine-design and initial evaluation. IEEE Trans Med Imag 21:991–997
6. Del Fabbro M, Taschieri (2010) Endodontic therapy using magnification devices: a systematic review. J Dent 38:269–275
7. Staudt C, Kinzel S, Hassfeld S, Stein W, Staehle H, Dörfer C (2001) Root canal morphology of permanent three-rooted mandibular first molars. Part 1: pulp floor and root canal system. J Clin Periodontol 28:746–752
8. J. Eberhart, M. Frentzen, and M. Thoms (2007) New method to detect caries via fluorescence. In: Schweitzer D, Fitzmaurice M (eds) Diagnostic Optical Spectroscopy in Biomedicine IV, Vol. 6628 of Proceedings of SPIE-OSA Biomedical Optics, Optical Society of America, Washington, paper 6628_21

9. Brüllmann D, Schmidtmann I, Warzecha K, d'Hoedt B (2011) Recognition of root canal orifices at a distance—a preliminary study of teledentistry. J Telemed Telecare 17:154–157
10. Krasner P, Rankow H (2004) Anatomy of the pulp-chamber floor. J Endod 30:5–16
11. Brüllmann D, Alvarez P, Willershausen B (2009) Recognition of root canal orifices in video sequences as a future support system during endodontic treatment. J Endod 35:1400–1403
12. Selvarasu N, Nachiappan A, Nandhitha N (2010) Abnormality detection from medical thermographs in human using euclidean distance based color image segmentation. IEEE Computer Society (ed) International Conference on Signal Acquisition and Processing, 2010. ICSAP '10, IEEE Computer Society, Los Alamitos, pp 73–75
13. Friedman J, Baskett F, Shustek L (1975) An algorithm for finding nearest neighbors. IEEE Trans Comput 24:1000–1006
14. Sun B, Du J, Gao T (2009) Study on the improvement of k-nearest neighbor algorithm. In: IEEE Computer Society (ed) International Conference on Artificial Intelligence and Computational Intelligence, 2009. AICI '09, IEEE Computer Society, Los Alamitos, pp 390–393
15. Knuth D (1998) The art of computer programming, 2nd edn., Addison Wesley, Bonn
16. Shim J, Dorai C (1999) A generalized region labeling algorithm for image coding, restoration and segmentation. In IEEE Computer Society (ed) International Conference on Image Processing, 1999. ICIP 99. Proceedings. IEEE Computer Society, Los Alamitos, pp 46–50
17. Jaehne B (2010) Digital image processing, 7st edn. Springer Berlin
18. Gu Y, Lu Q, Wang H, Ding Y, Wang P, Ni L (2010) Root canal morphologyof permanent three-rooted mandibular first molars. Part 1: pulp floor and root canal system. J Endod 36:990–994
19. de Menezes M, Rosati R, Ferrario V, Sforza C (2010) Accuracy and reproducibility of a 3-dimensional stereophotogrammetric imaging system. J Oral Maxillofac Surg 68:2129–2135
20. Rosati R, Menezes M, Rossetti A, Sforza C, Ferrario V (2010) Digital dental cast placement in 3-dimensional, full-face reconstruction: a technical evaluation. Am J Orthod Dentofacial Orthop 138:84–88
21. Wengert C, Cattin P, Du J, Baur C, Szekely G (2006) Markerless endoscopic registration and referencing. Med Image Comput Computer-Assist Interv 9:816–823